

**California Regional PM<sub>10</sub> and PM<sub>2.5</sub> Air Quality Study (CRPAQS)  
Data Analysis Task 1.1b  
EXAMINATION OF REACTIVE NITROGEN  
PARTITIONING AT THE BAKERSFIELD AND  
ANGIOLA FIELD SITES**

**TECHNICAL MEMORANDUM  
STI-902322-2652-TM2**

**By:**  
**Martin P. Buhr**  
**Erin Shields**  
**Elizabeth M. Simon**  
**Stephen B. Reid**  
**Sonoma Technology, Inc.**  
**1360 Redwood Way, Suite C**  
**Petaluma, CA 94954**

**Prepared for:**  
**California Air Resources Board**  
**1001 I Street**  
**Sacramento, CA 95814**

**July 29, 2005**



## **DISCLAIMER**

The statements and conclusions in this report are those of the Contractor and not necessarily those of the California Air Resources Board, the San Joaquin Valleywide Air Pollution Study Agency, or its Policy Committee, their employees or their members. The mention of commercial products, their source, or their use in connection with material reported herein is not to be construed as actual or implied endorsement of such products.



## TABLE OF CONTENTS

<u>Section</u>	<u>Page</u>
DISCLAIMER .....	iii
LIST OF FIGURES .....	vii
LIST OF TABLES .....	ix
1. INTRODUCTION.....	1-1
2. TECHNICAL APPROACH.....	2-1
3. RESULTS AND DISCUSSION .....	3-1
3.1 Data Included in the Analysis.....	3-2
3.1.1 NO Data.....	3-2
3.1.2 NO <sub>2</sub> Data .....	3-2
3.1.3 PAN Data .....	3-2
3.1.4 Nitrate Data .....	3-2
3.1.5 NO <sub>y</sub> Data .....	3-3
3.1.6 Ancillary Physical and Chemical Data.....	3-3
3.2 Comparison of Collocated Measurements.....	3-3
3.2.1 NO <sub>y</sub> .....	3-3
3.2.2 NO .....	3-5
3.2.3 Nitrate .....	3-6
3.3 NO <sub>y</sub> Partitioning .....	3-9
3.3.1 Individual Species .....	3-9
3.3.2 Diurnal Variation.....	3-12
3.4 NO <sub>y</sub> Partitioning as a Function of Other Physical and Chemical Parameters .....	3-15
3.4.1 Temperature.....	3-16
3.4.2 Ozone.....	3-18
3.4.3 Light Scattering .....	3-20
3.5 Data Quality Assessments .....	3-21
3.5.1 NO .....	3-22
3.5.2 NO <sub>2</sub> .....	3-22
3.5.3 PAN .....	3-22
3.5.4 Nitrate .....	3-22
3.5.5 NO <sub>y</sub> .....	3-22
4. SUMMARY .....	4-1
5. REFERENCES .....	5-1



## LIST OF FIGURES

<b><u>Figure</u></b>	<b><u>Page</u></b>
3-1. NO contribution to NO <sub>y</sub> measured at the Angiola site during different seasons. ....	3-1
3-2. Comparison of the collocated NO <sub>y</sub> measurements at the Sierra Nevada Foothills site. ....	3-4
3-3. Comparison of the collocated NO <sub>y</sub> measurements at the Angiola site. ....	3-4
3-4. Comparison of the collocated NO <sub>y</sub> measurements at the Fresno First Street site. ....	3-5
3-5. Comparison of the collocated NO measurements at the Fresno First Street site. ....	3-6
3-6. Comparison of the collocated nitrate measurements at the Sierra Nevada Foothills site. ....	3-7
3-7. Comparison of the collocated nitrate measurements at the Bethel Island site. ....	3-7
3-8. Comparison of the collocated nitrate measurements at the Bakersfield site. ....	3-8
3-9. Comparison of the collocated nitrate measurements at the Angiola site. ....	3-8
3-10. Contribution of the individual nitrogen species to NO <sub>y</sub> at the Sierra Nevada Foothills site. ....	3-12
3-11. Contribution of the individual nitrogen species to NO <sub>y</sub> at the Fresno First Street site. ....	3-12
3-12. Contribution of the individual nitrogen species to NO <sub>y</sub> at the Bethel Island site. ....	3-12
3-13. Contribution of the individual nitrogen species to NO <sub>y</sub> at the Bakersfield site. ....	3-12
3-14. Contribution of the individual nitrogen species to NO <sub>y</sub> at the Angiola site. ....	3-12
3-15. Diurnal variation of NO <sub>y</sub> partitioning at the Sierra Nevada Foothills site. ....	3-13
3-16. Diurnal variation of NO <sub>y</sub> partitioning at the Fresno First Street site. ....	3-13
3-17. Diurnal variation of NO <sub>y</sub> partitioning at the Bethel Island site. ....	3-14
3-18. Diurnal variation of NO <sub>y</sub> partitioning at the Bakersfield site. ....	3-14
3-19. Diurnal variation of NO <sub>y</sub> partitioning at the Angiola site. ....	3-15
3-20. Relationship observed between the individual species contribution to NO <sub>y</sub> and temperature at the Sierra Nevada Foothills site. ....	3-16

## LIST OF FIGURES (Concluded)

### **Figure Page**

3-21.	Relationship observed between the individual species contribution to NO <sub>y</sub> and temperature at the Fresno site. ....	3-17
3-22.	Relationship observed between the individual species contribution to NO <sub>y</sub> and temperature at the Bakersfield site.....	3-17
3-23.	Relationship observed between the individual species contribution to NO <sub>y</sub> and temperature at the Angiola site. ....	3-18
3-24.	Relationship observed between the individual species contribution to NO <sub>y</sub> and ozone at the Sierra Nevada Foothills site.....	3-19
3-25.	Relationship observed between the individual species contribution to NO <sub>y</sub> and ozone at the Fresno site.....	3-19
3-26.	Relationship observed between the individual species contribution to NO <sub>y</sub> and ozone at the Angiola site.....	3-20
3-27.	Relationship observed between the individual species contribution to NO <sub>y</sub> and light scattering at the Angiola site.....	3-21
3-28.	Relationship observed between the individual species contribution to NO <sub>y</sub> and light scattering at the Bethel Island site. ....	3-21



## LIST OF TABLES

<b><u>Table</u></b>	<b><u>Page</u></b>
2-1. Continuous nitrogen species measurements (and selected other continuous measurements) made at the Angiola, Bakersfield, Fresno, Bethel Island, and Sierra Nevada Foothills sites. ....	2-1
2-2. Time resolution of continuous nitrogen species measurements (and selected other continuous measurements) made at the Angiola, Bakersfield, Fresno, Bethel Island, and Sierra Nevada Foothills sites. ....	2-2



## 1. INTRODUCTION

Previous studies have indicated that, under many conditions, formation of aerosol nitrate in the San Joaquin Valley (SJV) depends on the availability of nitric acid. In turn, the formation of nitric acid depends on both the availability of precursors and the oxidative capacity of the atmosphere. This data analysis task is aimed at bettering our understanding of the reactive nitrogen partitioning observed during the California Regional PM<sub>10</sub> and PM<sub>2.5</sub> Air Quality Study (CRPAQS) measurement phase and relating variations in that partitioning to the coincident oxidative conditions. One of the first steps in this analysis is to assess the reliability of the various NO<sub>y</sub> components (nitric oxide (NO), nitrogen dioxide (NO<sub>2</sub>), peroxy acetyl nitrate (PAN), nitric acid (HNO<sub>3</sub>), and particulate nitrate, (collectively NO<sub>y(i)</sub>) that were measured. It is understood that PAN data will be available for a limited number of episodes and that HNO<sub>3</sub> data are not available from the Angiola core site. In addition, the NO<sub>2</sub> data that is available is limited in temporal coverage.

The objectives of this work were to address the following questions for the reactive nitrogen species:

1. What is the comparability and equivalence among collocated sampling methods, what are the biases of one instrument with respect to others, and how should these biases be minimized?
2. What is the quality of the NO<sub>y</sub> and NO<sub>y(i)</sub> species data collected? If some bias in the data is found, what utility might the data still have (e.g., establishing limits on the concentration of some species)?
3. How do the established data quality bounds limit the utility of the reactive nitrogen data to illustrate the chemical and physical processes that link the primarily gas-phase reservoir of reactive nitrogen to particulate matter (PM) concentration issues?



## 2. TECHNICAL APPROACH

Continuous measurements of NO<sub>y</sub> and a number of nitrogen species components were made at the anchor sites during the CRPAQS winter measurement period. We evaluated these measurements and characterized the partitioning among these species by making various comparisons as a function of site, time of day, and other chemical and physical characteristics. This data analysis task is aimed at evaluating and documenting the quality of the reactive nitrogen species measurements and improving our understanding of the reactive nitrogen partitioning observed during the CRPAQS measurement phase and relating variations in that partitioning to the coincident oxidative conditions. The results of this task will serve to establish qualitative confidence limits on the evaluation of processes leading to the formation of particulate nitrate from its precursor species.

### Data Availability

Continuous air quality data was collected for a number of reactive nitrogen species at the anchor sites during the winter measurement periods, typically mid-November 2000 through mid-February 2001 (see **Table 2-1**). These measurements include NO<sub>y</sub> and its major components NO, NO<sub>2</sub>, PAN, nitric acid, and aerosol nitrate. All these measurements were made at a time resolution of 5 or 10 minutes (see **Table 2-2**). Tables 2-1 and 2-2 also show the data availability and time resolution of several additional parameters that might influence the nitrogen species partitioning including ozone, PM<sub>2.5</sub> and PM<sub>10</sub> mass, and light scattering. Evaluation of the reactive nitrogen budget required integration of the NO, NO<sub>2</sub>, PAN, HNO<sub>3</sub>, and NO<sub>y</sub> measurements over the sample period of the nitrate measurement.

Table 2-1. Continuous nitrogen species measurements used in this analysis (and selected other continuous measurements) made at the Angiola, Bakersfield, Fresno, Bethel Island, and Sierra Nevada Foothills sites.

ID	Site Instrument	Angiola	Bakersfield	Fresno First Street	Bethel Island	Sierra Nevada Foothills
A	Nephelometer	2/1/00–2/16/01	1/27/00–4/18/01	12/1/99–2/1/01	11/15/00–2/15/01	11/2/00–2/8/01
G	Aethalometer	1/12/00–3/29/01	1/20/00–2/19/01	12/1/99–2/1/01	11/17/00–2/15/01	11/19/00–2/14/01
J	PM <sub>10</sub> BAM <sup>a</sup>	1/21/00–3/29/01	1/21/00–4/9/01	12/1/99–2/1/01	-	11/19/00–2/12/01
K	PM <sub>2.5</sub> BAM <sup>a</sup>	1/21/00–3/29/01	1/21/00–4/18/01	12/1/99–2/1/01	11/17/00–2/15/01	11/19/00–2/12/01
N	PAN/NO <sub>2</sub>	11/19/00–2/12/01	10/11/00–2/12/01	12/10/00–2/1/01	11/22/00–2/12/01	11/10/00–2/13/01
O	NO <sub>y</sub>	12/20/99–2/23/01	12/16/99–3/26/01	12/1/99–2/1/01	11/18/00–2/15/01	11/16/00–2/15/01
P	O <sub>3</sub>	1/22/00–2/21/01	Ongoing (ARB) <sup>c</sup>	Ongoing (ARB) <sup>c</sup>	Ongoing (BAAQMD) <sup>b</sup>	11/3/00–2/13/01
Q	Nitrate	11/19/00–3/2/01	11/15/00–3/6/01	11/13/00–2/10/01	11/28/00–2/6/01	11/20/00–2/12/01
R	HNO <sub>3</sub>	11/21/00–2/26/01	–	11/30/00–2/1/01	–	11/16/00–2/15/01

<sup>a</sup> Beta Attenuation Monitor

<sup>b</sup> Bay Area Air Quality Management District

<sup>c</sup> California Air Resources Board

Table 2-2. Time resolution of continuous nitrogen species measurements (and selected other continuous measurements) made at the Angiola, Bakersfield, Fresno, Bethel Island, and Sierra Nevada Foothills sites.

ID	Instrument	Time Resolution (minutes)
A	Nephelometer	5, 60
G	Aethalometer	5, 60
J	PM <sub>10</sub> BAM	60
K	PM <sub>2.5</sub> BAM	60
N	PAN/NO <sub>2</sub>	5, 60
O	NO <sub>y</sub>	5, 60
P	O <sub>3</sub>	5, 60
Q	Nitrate	10, 60
R	HNO <sub>3</sub>	5, 60

The primary focus of this analysis was to make an assessment of the reliability of the NO<sub>y</sub> measurements. For example, we compared the NO<sub>y</sub> measured by the NO/NO<sub>y</sub> monitor with the NO<sub>y</sub> measured by the nitric acid monitor. Consistency between these two NO<sub>y</sub> measurements will promote confidence in the nitric acid measurements. We conducted NO<sub>y</sub> comparisons for each site and for various times during the CRPAQS winter measurement periods to evaluate the comparability of the two NO<sub>y</sub> measurements. Any bias discovered between the collocated measurements of NO<sub>y</sub> will help to establish uncertainty bounds for subsequent evaluation of the reactive nitrogen budget.

Next, the other NO<sub>y</sub> species measured (PAN, HNO<sub>3</sub>, particulate nitrate) were examined primarily in relationship to their contribution to NO<sub>y</sub>. This examination of the reactive nitrogen reservoir can be helpful in describing the dynamic and chemical history of an air mass (Buhr et al., 1990; Trainer et al., 1991). Finally, the ratio  $\Sigma\text{NO}_{y(i)}/\text{NO}_y$  will be examined to determine the overall consistency of the reactive nitrogen species data set.

Further analysis incorporated other chemical and physical parameters as needed to generate a better understanding of the conditions that lead to formation particulate nitrate.

### 3. RESULTS AND DISCUSSION

The measurements collected during the CRPAQS experiment that lend themselves to a detailed examination of reactive nitrogen partitioning are limited to the winter intensive portion of the operations, nominally December 1, 2000 through February 15, 2001. Those measurements included  $\text{NO}_y$  (total reactive nitrogen measured with a heated molybdenum converter),  $\text{NO}$ ,  $\text{NO}_2$  (measured using a gas chromatograph and luminol chemiluminescence detector), PAN (also measured with the luminol detector-based gas chromatograph), particulate nitrate (measured both with a continuous method and via filter-based discrete sampling), and  $\text{HNO}_3$  (measured using the discrete filter samples). While the winter period was clearly the most important to understand from the perspective of particulate nitrate formation, it is useful to understand the differences observed between the seasons to better understand the driving forces behind reactive nitrogen oxidation.

**Figure 3-1** shows the diurnal variation of the  $\text{NO}/\text{NO}_y$  ratio observed at the Angiola field site during each of the CRPAQS intensives. Among the notable features of this plot is the progression toward higher morning maxima going from summer through fall to winter, and the lower afternoon/evening ratio in the summertime measurements. While it is possible that there is a seasonal difference in the valley-wide source strength of  $\text{NO}$  emissions, most of the differences observed can be attributed to a combination of greater vertical mixing, and thus greater dilution, during the summer months; and greater photochemical activity leading to the conversion of  $\text{NO}$  to more oxidized  $\text{NO}_y$  species.

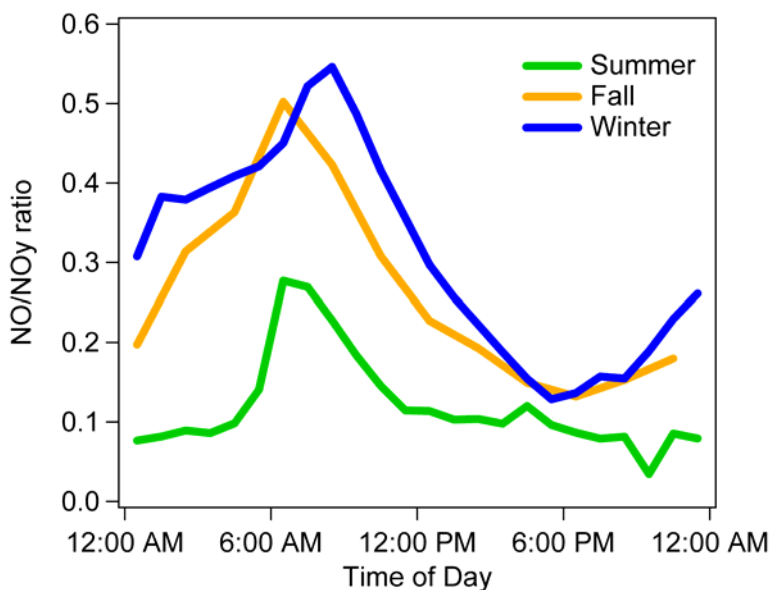


Figure 3-1.  $\text{NO}$  contribution to  $\text{NO}_y$  measured at the Angiola site during different seasons.

The same factors, dynamics and chemistry, affect the shape of the fall and winter diurnal profiles. Examination of the other reactive nitrogen species contribution to  $\text{NO}_y$  during the

winter intensive can serve as a starting point for separating these effects and thereby lead to a greater understanding of the processes that lead to nitrate particle formation. The analysis presented here focuses on understanding the quality of the reactive nitrogen data collected through examination of the correlation of collocated samplers, the absolute and diurnal behavior of the individual species contributions to  $\text{NO}_y$ , and through a qualitative examination of the dependence of that contribution on other chemical and physical factors.

### **3.1 DATA INCLUDED IN THE ANALYSIS**

The data included in the analysis were the  $\text{NO}$ ,  $\text{NO}_2$ , PAN, nitrate,  $\text{HNO}_3$ , and  $\text{NO}_y$  measurements available in the Central California Air Quality Studies (CCAQS) database in the early spring of 2004 from the Sierra Nevada Foothills (SNF), Bethel Island (BTI), Fresno First Street (FSF), Bakersfield (BAC), and Angiola (ANG) anchor sites. For the purposes of this evaluation the data were integrated over the slowest time base, in this case the filter nitrate measurements. For most of the field sites this resulted in approximately 75 integrated samples. There were some differences in the methods used for the various species measurements at the different sites so it is useful to examine those methods explicitly at the onset of the analysis.

#### **3.1.1 NO Data**

The  $\text{NO}$  data collected at all of the sites was performed using  $\text{NO}+\text{O}_3$  chemiluminescence instruments.

#### **3.1.2 $\text{NO}_2$ Data**

The  $\text{NO}_2$  data collected at the ANG, BAC, SNF, and BTI sites was performed using a combination gas chromatograph/luminol chemiluminescence instrument. The  $\text{NO}_2$  measurement performed at the FSF site was based on the difference in signal between the internal catalytic converter of a  $\text{NO}+\text{O}_3$  chemiluminescence instrument.

#### **3.1.3 PAN Data**

The PAN data collected at the ANG, BAC, SNF, and BTI sites was performed using the same combination gas chromatograph/luminol chemiluminescence instrument used for the  $\text{NO}_2$  measurements at those sites. There were no PAN measurements collected at the FSF site.

#### **3.1.4 Nitrate Data**

Particulate nitrate measurements were performed using two different systems at each of sites. First, discrete filter samples were collected at each of the sites over the course of two to six hours for a total of five samples per day during the intensive operation periods (IOPs) of the winter intensive. In addition, at each of the sites there were continuous nitrate analyzers based on flash vaporization of particle samples impinged on a metal strip, followed by analysis using



an NO+O<sub>3</sub> chemiluminescence instrument. The data from the continuous instrument at the FSF site was not available at the time this analysis was performed.

### 3.1.5 NO<sub>y</sub> Data

NO<sub>y</sub> data was collected at each of the sites using an inlet-mounted, heated molybdenum catalytic converter followed by an NO+O<sub>3</sub> chemiluminescence instrument. In theory, the catalytic converter should convert all of the individual NO<sub>y</sub> species to NO. In practice, the NO<sub>y</sub> instrument at FSF was operated with an inlet filter, so that particular NO<sub>y</sub> measurement should represent NO<sub>y</sub> less the portion of the particulate nitrate trapped on the inlet filter.

### 3.1.6 Ancillary Physical and Chemical Data

Additional measurements collected at each of the sites that were used in this analysis include ozone, light scattering, temperature, and relative humidity. However, not all of these ancillary parameters were available for all of the IOPs included in the analysis.

## 3.2 COMPARISON OF COLLOCATED MEASUREMENTS

The first order evaluation of the reactive nitrogen measurements was comparison of the collocated measurement results. These include NO<sub>y</sub> at the ANG, SNF, and FSF sites; NO at the FSF site; and continuous versus filter nitrate at all of the sites except for FSF.

### 3.2.1 NO<sub>y</sub>

Comparison of the collocated NO<sub>y</sub> measurements is particularly important since most of the analysis presented here is predicated on the understanding that we have an accurate measurement of NO<sub>y</sub>. That said, in each case the NO<sub>y</sub> comparisons are made using essentially identical systems and any systematic or functional design error could influence both systems. The results of the comparison for the collocated systems at SNF, ANG, and FSF are shown in **Figures 3-2 through 3-4**. The comparisons from both SNF and ANG show excellent agreement (<10% difference from unity). At the least, this suggests that the measurement systems were operated in a consistent fashion, and, at most, suggests that the NO<sub>y</sub> measurement systems actually measure NO<sub>y</sub>. The comparison observed at the FSF site is markedly worse, but for understandable reasons. It is critical to note that the data represented by value\_NOyNOy in Figure 4 were from the standard NO<sub>x</sub> instrument that used an internal, rather than inlet-mounted catalytic NO<sub>y</sub> converter. It is expected that this difference contributes significantly to the poor correlation seen between the two measurement systems.

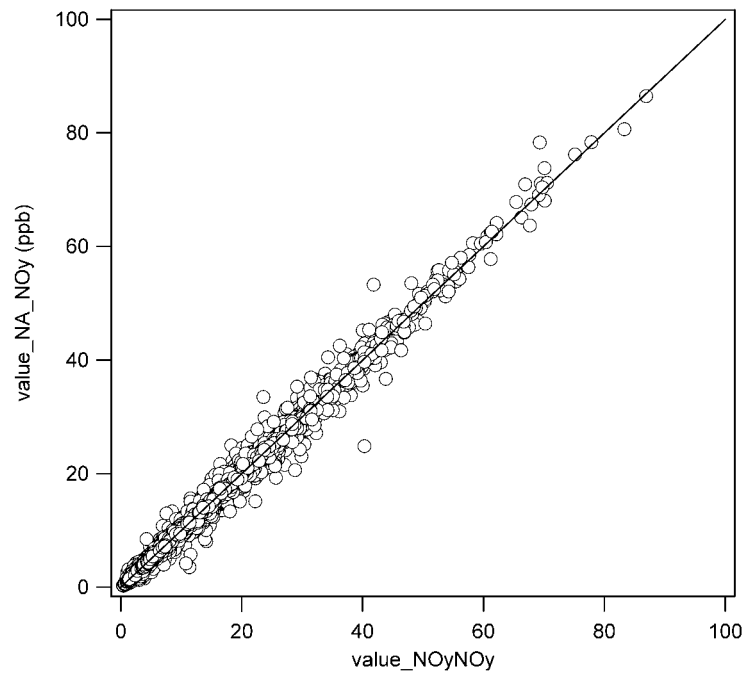


Figure 3-2. Comparison of the collocated NO<sub>y</sub> measurements at the Sierra Nevada Foothills site.

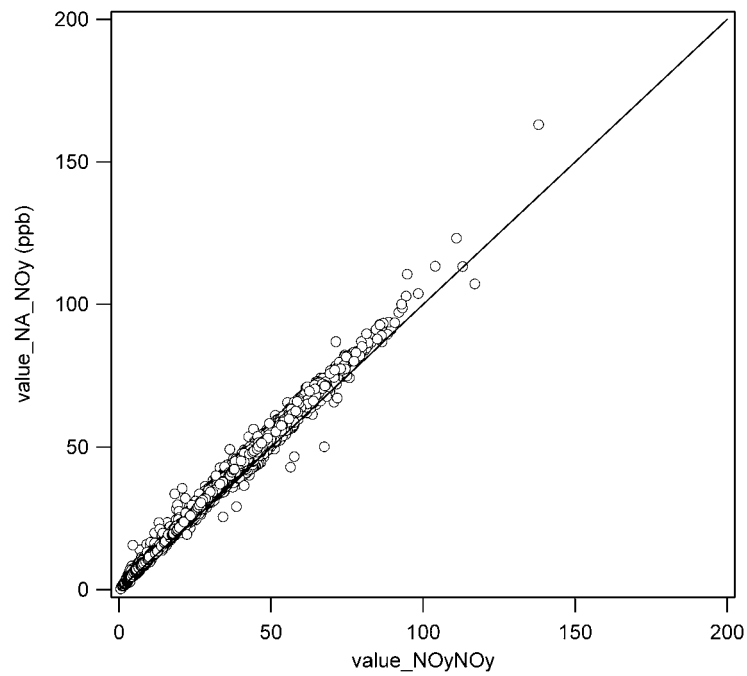


Figure 3-3. Comparison of the collocated NO<sub>y</sub> measurements at the Angiola site.

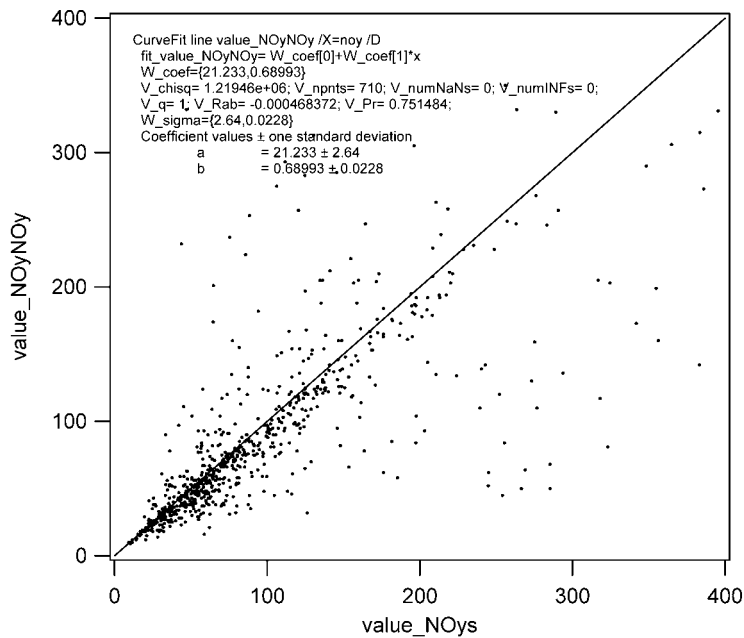


Figure 3-4. Comparison of the collocated NO<sub>y</sub> measurements at the Fresno First Street site.

### 3.2.2 NO

In addition to the different NO<sub>y</sub> measurements reported from the FSF site, two different NO measurements were reported as well. These data are shown in **Figure 3-5**. The comparison between the separate NO measurements was considerably better than the separate NO<sub>y</sub> measurements from the same instruments. The  $r^2$  for the NO measurements was 0.75 versus  $r^2=0.56$  for the NO<sub>y</sub> measurements. While this does not lend much confidence to the NO measurements it is possible that part of the disparity resulted from calibration differences since the standard system was operated by CARB and the custom system was operated by Desert Research Institute (DRI).

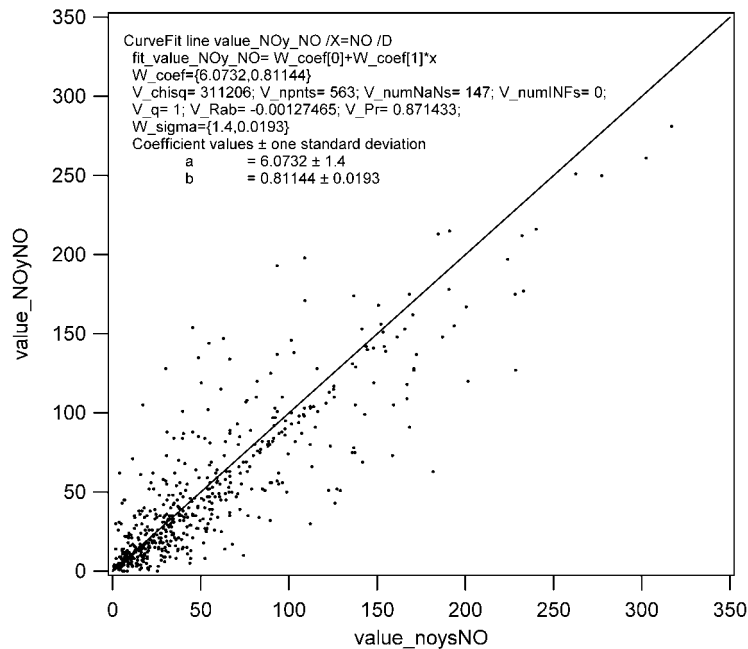


Figure 3-5. Comparison of the collocated NO measurements at the Fresno First Street site.

### 3.2.3 Nitrate

The comparisons of the collocated nitrate measurements for each of the sites except FSF are shown in **Figures 3-6 through 3-9**. The continuous nitrate measurement was low across the board, relative to the filter-based measurement with the least disparity observed at the BAC site and the greatest disparity observed at the Angiola site. It has been suggested that the continuous nitrate measurements tend towards either under sampling or particle loss (Hering, 2004), which may explain some of the difference observed. It is possible that the sampling loss was less pronounced at the Bakersfield site, resulting in the better correlation between the continuous and filter measurements. The agreement between the two methods is best at low concentrations with deviations at higher levels of 10-50%. For the purposes of understanding the relationship between the sum of the reactive nitrogen species and  $\text{NO}_y$ , the filter-based measurements were used except for the ANG data where both quantities were calculated.

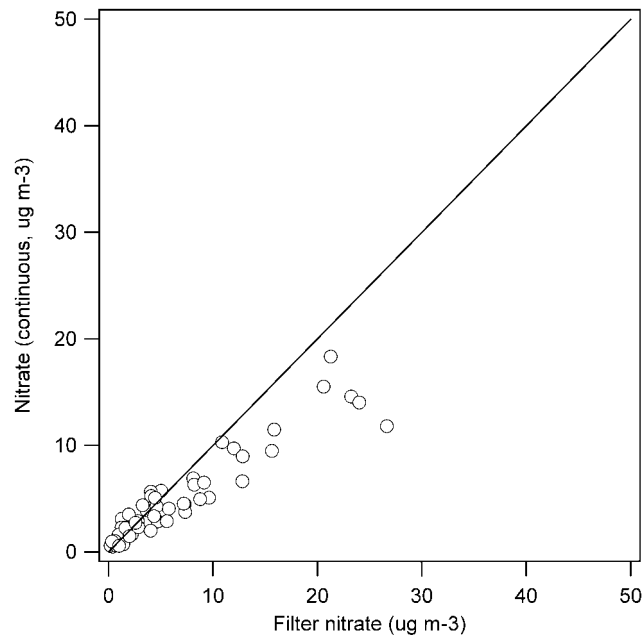


Figure 3-6. Comparison of the collocated nitrate measurements at the Sierra Nevada Foothills site.

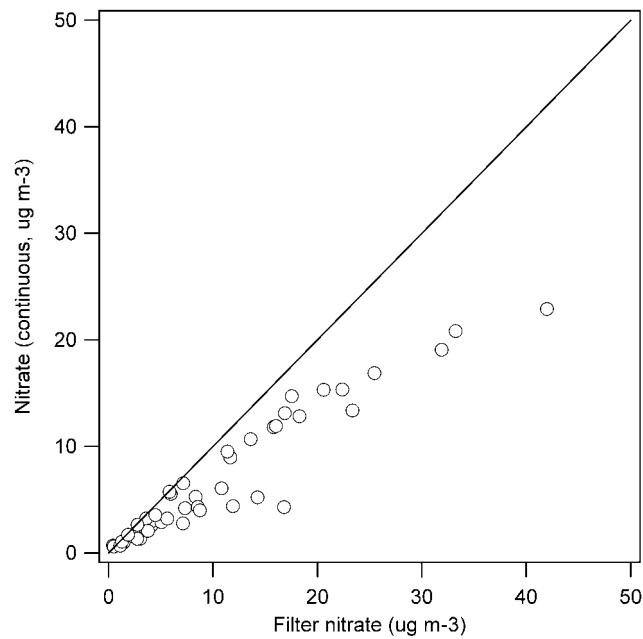


Figure 3-7. Comparison of the collocated nitrate measurements at the Bethel Island site.

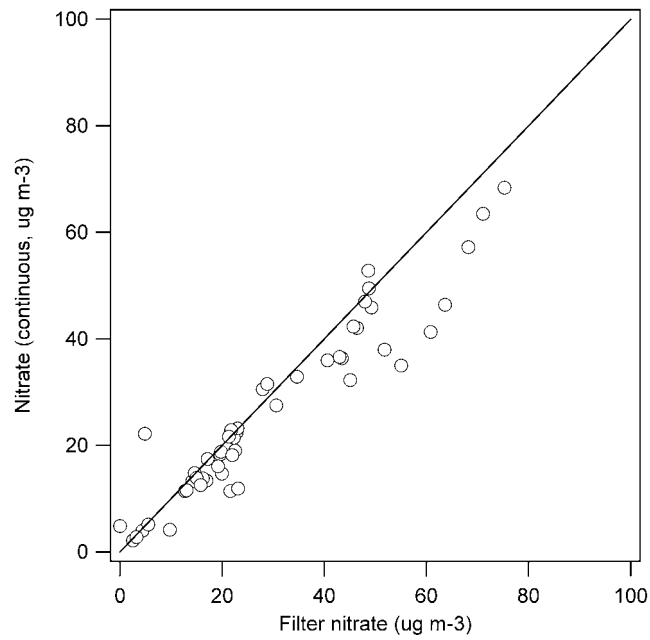


Figure 3-8. Comparison of the collocated nitrate measurements at the Bakersfield site.

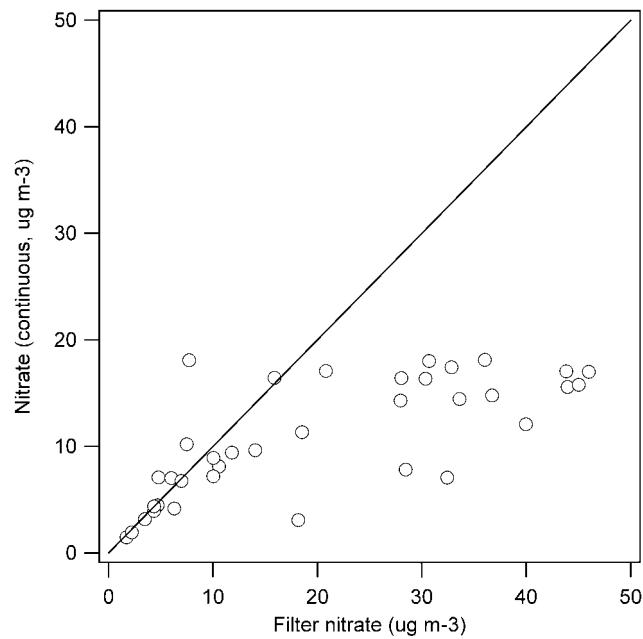


Figure 3-9. Comparison of the collocated nitrate measurements at the Angiola site.

### 3.3 NO<sub>y</sub> PARTITIONING

#### 3.3.1 Individual Species

A comparison of the individual NO<sub>y</sub> species to NO<sub>y</sub> is presented for each of the sites in **Figures 3-10 through 3-14**. It is important to note that for the FSF site (Figure 3-11) there are no PAN or continuous nitrate data and the data points indicated for those species are at zero value for that reason. These correlation plots were examined qualitatively from the perspective of correlation of the individual species with NO<sub>y</sub> and quantitatively from the perspective of absolute contribution to NO<sub>y</sub>. In connection with the latter, NO<sub>2</sub> was observed to exceed NO<sub>y</sub> periodically at the SNF and BTI sites. Since this is not physically possible, the observation suggests that either the NO<sub>y</sub> measurements at these sites were biased low or, more likely as discussed below, the NO<sub>2</sub> measurements at these sites were biased high.

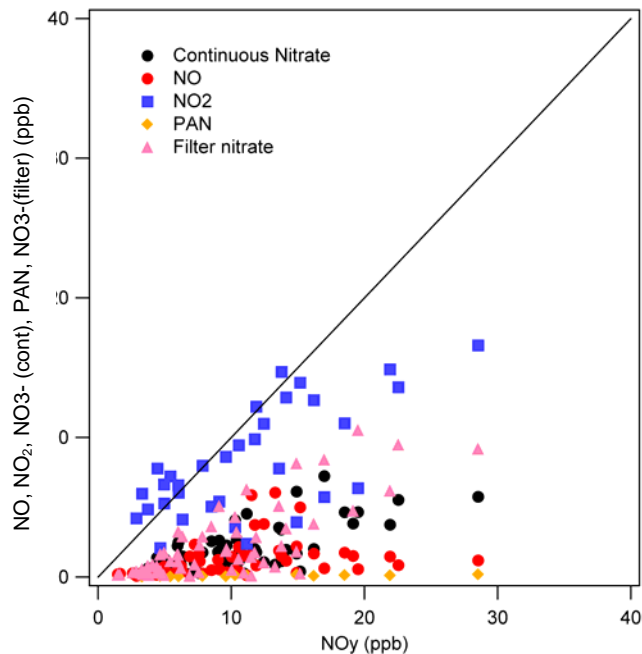


Figure 3-10. Contribution of the individual nitrogen species to NO<sub>y</sub> at the Sierra Nevada Foothills site.

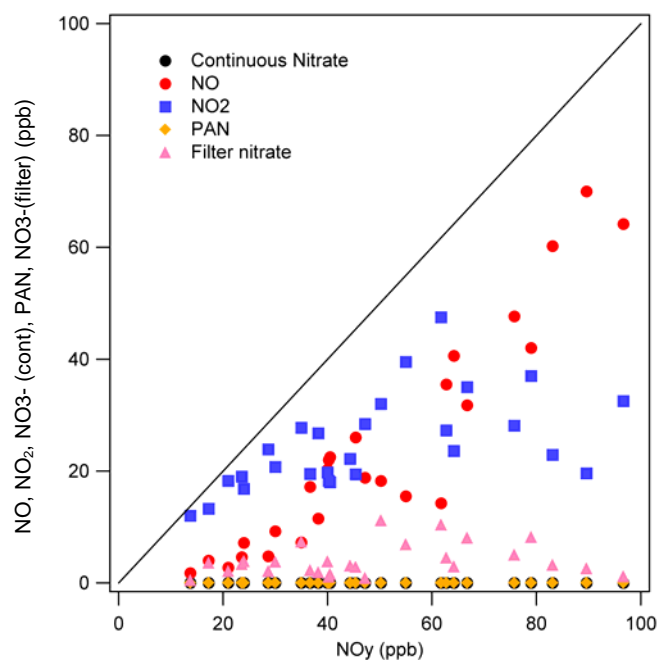


Figure 3-11. Contribution of the individual nitrogen species to  $\text{NO}_y$  at the Fresno First Street site.

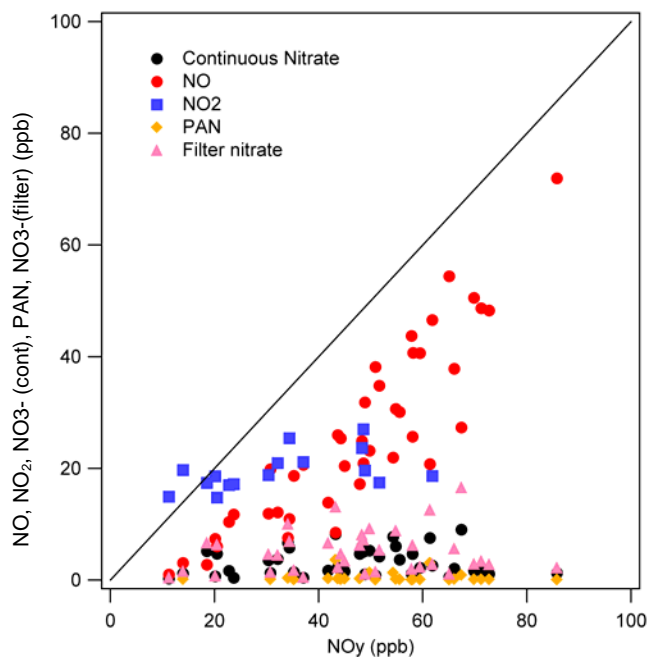


Figure 3-12. Contribution of the individual nitrogen species to  $\text{NO}_y$  at the Bethel Island site.



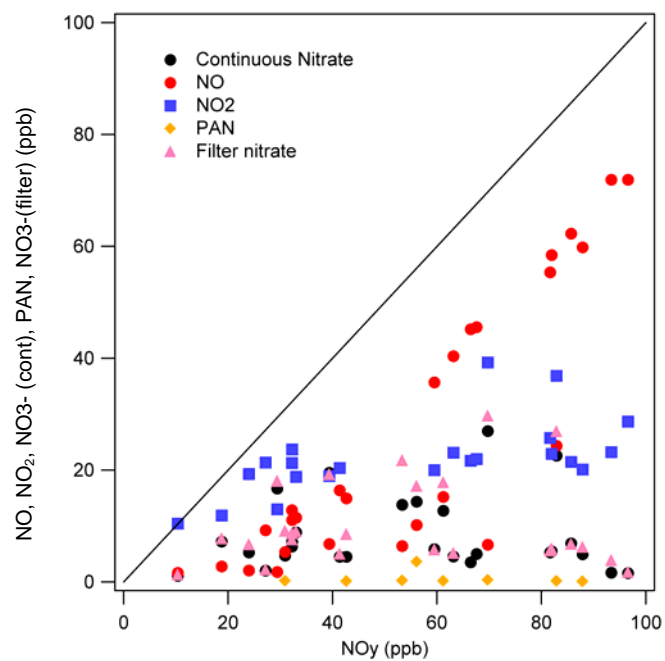


Figure 3-13. Contribution of the individual nitrogen species to  $\text{NO}_y$  at the Bakersfield site.

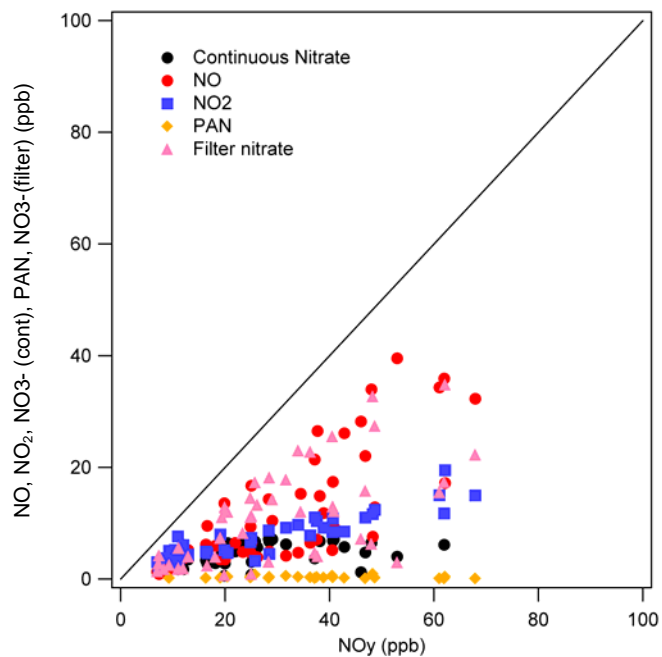


Figure 3-14. Contribution of the individual nitrogen species to  $\text{NO}_y$  at the Angiola site.

Despite the occasional apparent overestimates of the individual species, there is good correlation between the individual species and  $\text{NO}_y$ , with the possible exception of the  $\text{NO}_2$  measurements collected at the SNF and BTI sites, where only moderate correlation is observed. Examination of these data suggests that the  $\text{NO}_2$  measurements at these sites may have an unaccounted-for positive offset. In the next section it will become more evident that the  $\text{NO}_2$  concentration measured at BTI and SNF probably accounts for the  $\text{NO}_y$  species imbalance observed overall for these sites.

### 3.3.2 Diurnal Variation

Examination of the average diurnal variation of the  $\text{NO}_y(i)/\text{NO}_y$  ratio provides significant insight into how the individual species contribute to  $\text{NO}_y$  at a given site. **Figures 3-15 through 3-19** present this data for the sites examined. Included on each plot is the diurnal variation of  $\Sigma\text{NO}_y(i)/\text{NO}_y$ . For this analysis, the filter-based nitrate measurement, converted to ppbv assuming standard temperature and pressure, was used in calculation of the sum. Comparison of the pattern of  $\Sigma\text{NO}_y(i)$  with that of the individual species is particularly instructive for gaining an understanding of which species may be responsible for any overestimates of  $\text{NO}_y$  by  $\Sigma\text{NO}_y(i)$ .

Figure 3-15 presents the data collected at the SNF site. On average, the  $\Sigma\text{NO}_y(i)$  overestimates the observed  $\text{NO}_y$  by more than 20%. The individual contributions shown in Figure 3-15 suggest that the  $\text{NO}_2$  concentration may be grossly overestimated. This is supported by the observation that  $\text{NO}_2$  alone accounts for more than  $\text{NO}_y$  during many periods and the variation of  $\text{NO}_2/\text{NO}_y$  is quite similar to  $\Sigma\text{NO}_y(i)/\text{NO}_y$ . The physical impossibility of this indicates that the  $\text{NO}_2$  observations collected at SNF should be viewed as gross overestimates. The filter and continuous nitrate measurements at SNF are comparable in contribution to  $\text{NO}_y$  and show a distinct diurnal trend with a midday maximum. It is likely that the nitrate diurnal profile results from transport processes. Given that the  $\text{NO}_2$  measured at the SNF site was overestimated, the true contribution of the other species would be relatively higher.

The data presented in Figure 3-16 for the FSF site shows excellent balance between  $\text{NO}_y$  and  $\Sigma\text{NO}_y(i)$ . In part this is due to the fact that the  $\text{NO}_2$  measurement is calculated by the difference between an internal catalytic converter and NO measured with the same instrument. That said, if this measure of  $\text{NO}_2$  is in error it will be higher than the true value rather than lower. This contention is supported by the observation that the  $\text{NO}_2$  contribution increases during the middle of the day while we expect it to decrease due to photochemical activity. Nonetheless, the  $\Sigma\text{NO}_y(i)$  value is within 10% of unity on average. It is important to note that the measured  $\text{HNO}_3$  contribution to  $\text{NO}_y$  is not included in the sum ( $\text{HNO}_3$  was not included to provide consistency with the sites that do not have this measurement). Separate analysis indicates that the  $\text{HNO}_3$  contribution is on the order of 4% and does not significantly impact the  $\Sigma\text{NO}_y(i)$  value.

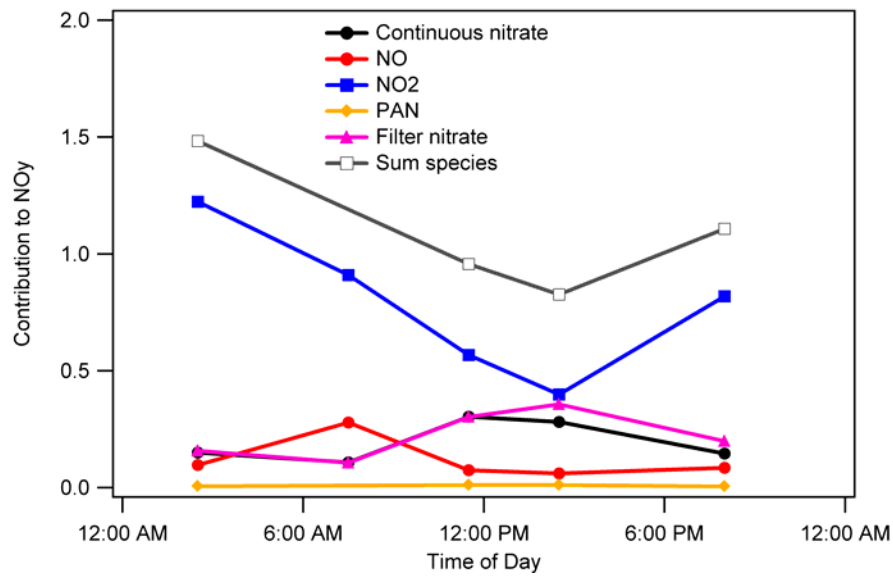


Figure 3-15. Diurnal variation of  $\text{NO}_y$  partitioning at the Sierra Nevada Foothills site.

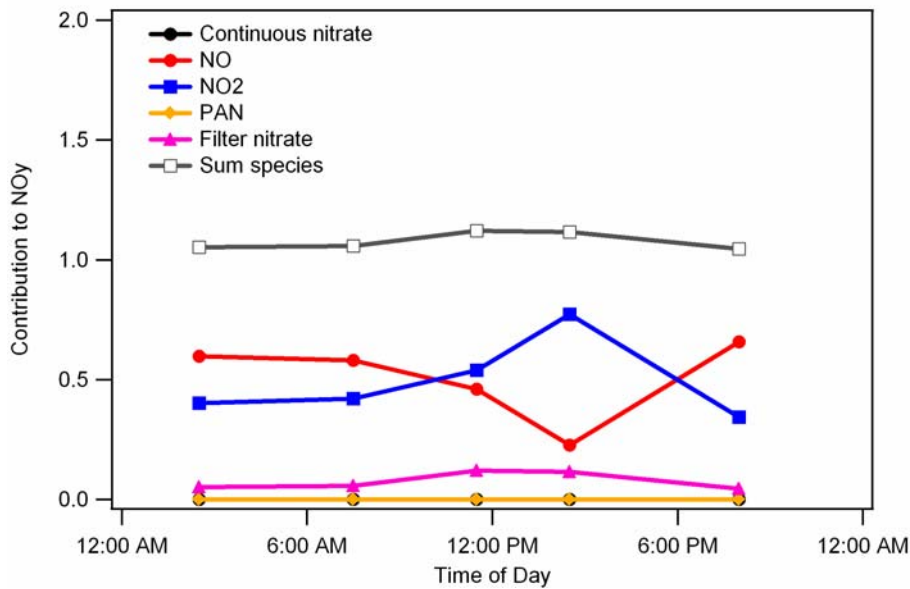


Figure 3-16. Diurnal variation of  $\text{NO}_y$  partitioning at the Fresno First Street site.

The data shown in Figure 3-17 represent the diurnal  $\text{NO}_y$  partitioning at the BTI site. The data from BTI are quite similar to those observed at SNF, including both the gross overestimate of  $\Sigma\text{NO}_y(i)$ , overestimated by 30% on average, and the probable contribution of  $\text{NO}_2$  to that overestimate.

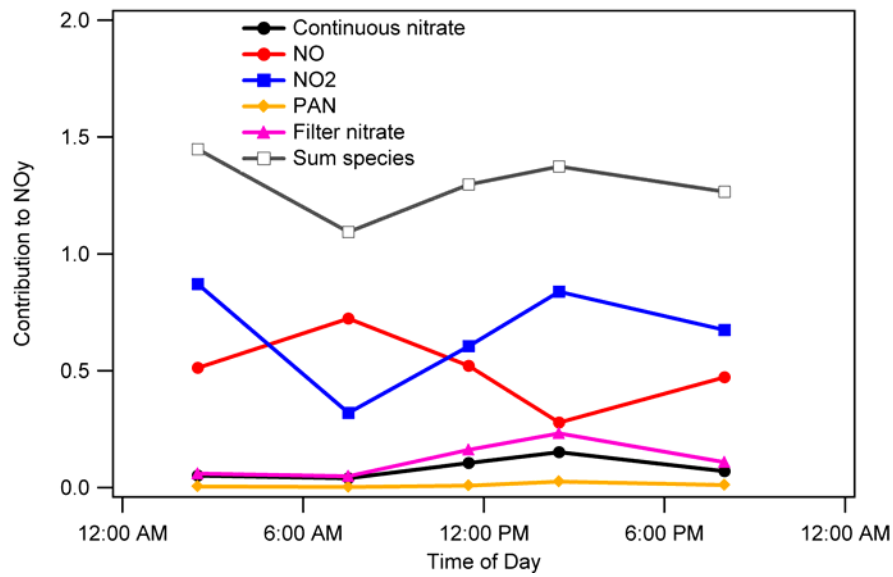


Figure 3-17. Diurnal variation of  $\text{NO}_y$  partitioning at the Bethel Island site.

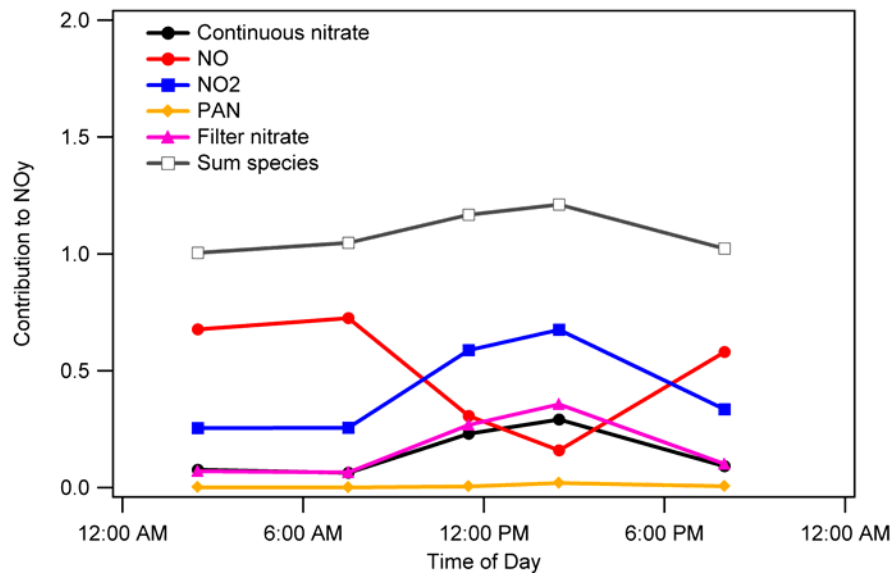


Figure 3-18. Diurnal variation of  $\text{NO}_y$  partitioning at the Bakersfield site.

The data shown in Figure 3-18 represent the diurnal  $\text{NO}_y$  partitioning observed at the BAC site. Our expectation is that the contribution to  $\text{NO}_y$  from nitrate should increase during the day due to photochemical processes while at the same time the contribution from  $\text{NO}_2$  should probably decrease during the day for the same reasons. Thus we submit that it is the  $\text{NO}_2$  contribution that drives the quantity  $\Sigma\text{NO}_y(i)$  out of balance during the daytime hours. That said, the  $\text{NO}_y$  balance at BAC is within 10% of unity on average.

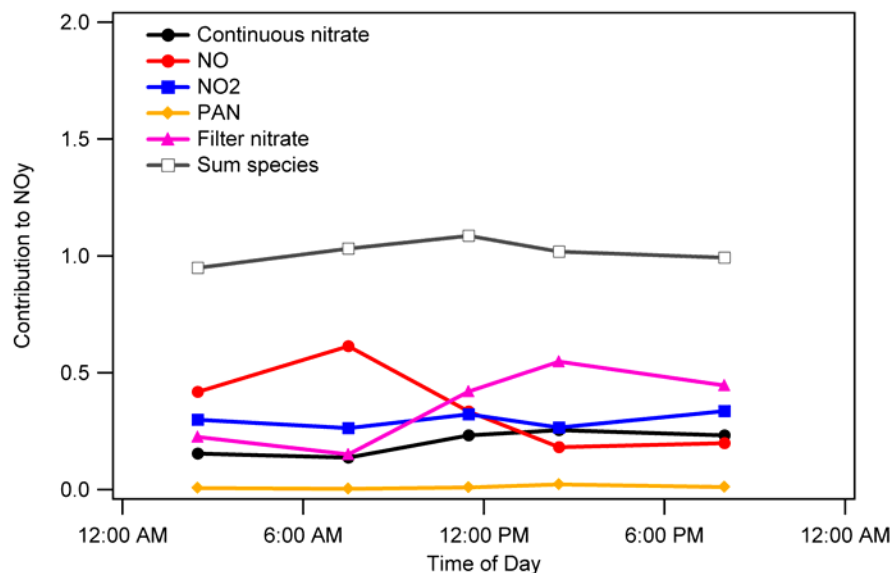


Figure 3-19. Diurnal variation of NO<sub>y</sub> partitioning at the Angiola site.

The data shown in Figure 3-19 represent the diurnal NO<sub>y</sub> partitioning observed at the ANG site. Different than the other sites, the NO<sub>2</sub> contribution at ANG is relatively low (~30%) and shows the expected decrease during the daytime hours. The unique features at ANG is the large contribution of filter nitrate to the total NO<sub>y</sub> budget and the disparity between the filter and continuous nitrate measurements. As was discussed in Section 3.2.3, the filter nitrate is often as much as twice as high as the continuous nitrate. The large contribution of nitrate to NO<sub>y</sub> at this site may be due to the longer photochemical processing times associated with this more regional site. This contention is supported by the persistence of the nitrate peak into the last sampling period. The other regional sites, SNF and BTI, would likely show a nitrate contribution similar to ANG if the data from those sites were not skewed by the overestimated NO<sub>2</sub> contribution. The NO<sub>y</sub> balance measured at the ANG site was the best observed, being within a few percent unity, on average.

### 3.4 NO<sub>y</sub> PARTITIONING AS A FUNCTION OF OTHER PHYSICAL AND CHEMICAL PARAMETERS

The analysis presented thus far has focused on the internal consistency of the reactive nitrogen measurements. In this section the analysis will be extended to examine the species contribution to NO<sub>y</sub> as a function of other chemical and physical parameters including temperature, ozone, and light scattering. On one hand this analysis could be useful in furthering our understanding of particulate nitrate formation. However, in this analysis we will examine the relationships observed in a qualitative sense to better understand the disparities observed in the reactive nitrogen balance. Inclusion of the continuous nitrate measurements in this analysis was performed for both consistency and for the possibility that a better understanding of the probable sampling issues would be elucidated.

### 3.4.1 Temperature

Figures 3-20 through 3-23 show the relationship between the  $\text{NO}_y(i)/\text{NO}_y$  ratio as a function of ambient temperature for the SNF, FSF, BAC, and ANG sites. In general, the strongest relationship we might expect to see is a negative, though not necessarily linear, relationship between nitrate and temperature. There is not strong evidence for this relationship with the possible exception of the ANG data (Figure 3-23). However, in the same data we also see increasing nitrate with increasing temperature. The BAC nitrate data (Figure 3-22) also show an increase in nitrate with increasing temperature. In both cases the relationship suggests an artifact, possibly due to temperature differentials between the ambient and enclosure environments. One conceivable phenomenon is off-gassing/release of  $\text{HNO}_3$  or  $\text{HNO}_3$  bearing particles from the sample inlet piping as the piping warms up either in the ambient or enclosure environment. The increase in nitrate with increasing temperature may also be due mixing down of aloft nitrate. Finally, it is notable that most of the sites show a decrease in NO with increasing temperature which may be understood to result from both increased mixing (dilution) and increased photochemistry with the warmer ambient temperature.

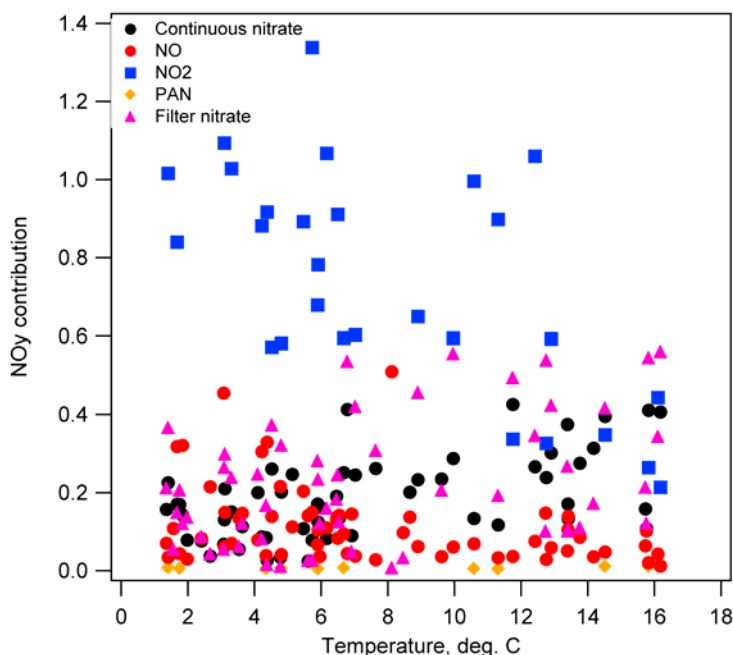


Figure 3-20. Relationship observed between the individual species contribution to  $\text{NO}_y$  and temperature at the Sierra Nevada Foothills site.

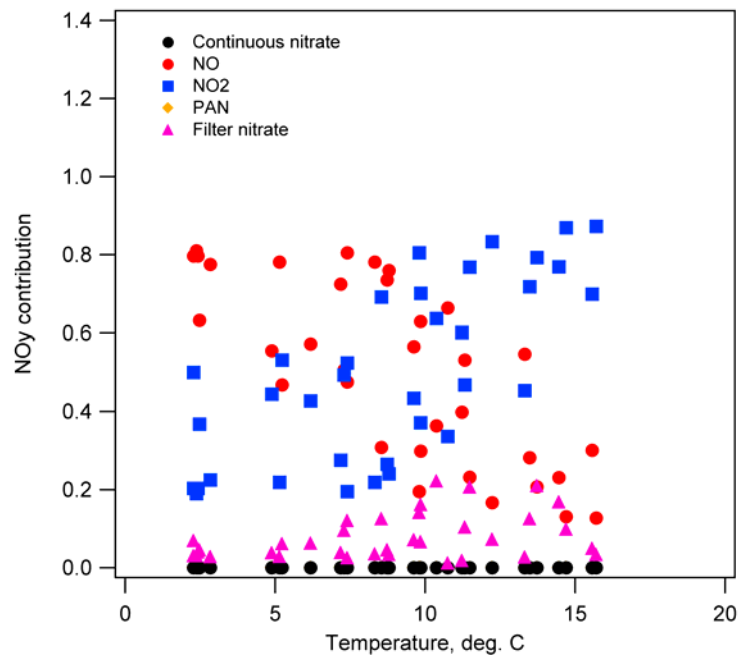


Figure 3-21. Relationship observed between the individual species contribution to  $\text{NO}_y$  and temperature at the Fresno site.

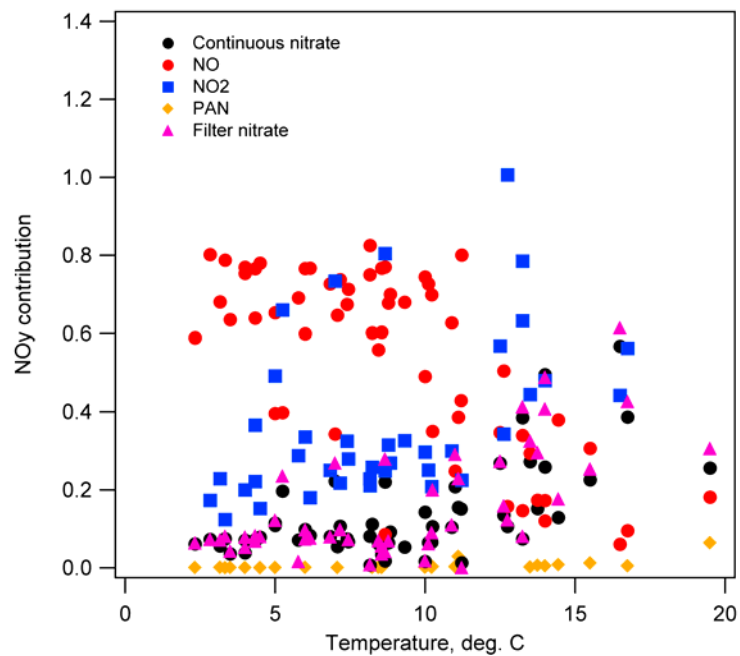


Figure 3-22. Relationship observed between the individual species contribution to  $\text{NO}_y$  and temperature at the Bakersfield site.

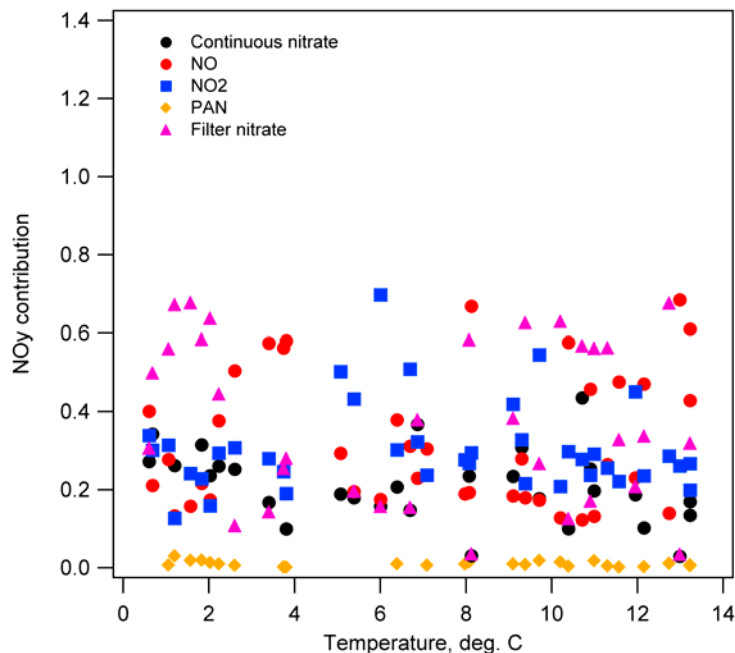


Figure 3-23. Relationship observed between the individual species contribution to  $\text{NO}_y$  and temperature at the Angiola site.

### 3.4.2 Ozone

Figures 3-24 through 3-26 show the relationship observed between the  $\text{NO}_y(i)$  species and ozone observed at the SNF, FSF and ANG sites. Focusing again on the nitrate/ $\text{NO}_y$  ratio, there may be arguments for either correlation between ozone and nitrate (common photochemical heritage), or anti-correlation (lower temperatures favor nitrate lifetime while tempering ozone formation). In either case, it is remarkable to see both correlation and anti-correlation with ozone from the two separate measures of nitrate collected at the ANG site (Figure 3-26). The continuous nitrate data decrease with increasing ozone while the filter nitrate data show a strong positive relationship. It is not clear what the cause of either relationship is, but the strength of the filter nitrate relationship with ozone suggests that this measurement suffered from an artifact related to some aspect of the chemical or physical framework that supported the photochemical conditions. The data from SNF show a weak positive relationship between nitrate contribution and ozone. The data from the FSF site show an expected relationship between NO,  $\text{NO}_2$  and ozone, but little, if any, relationship between nitrate and ozone.



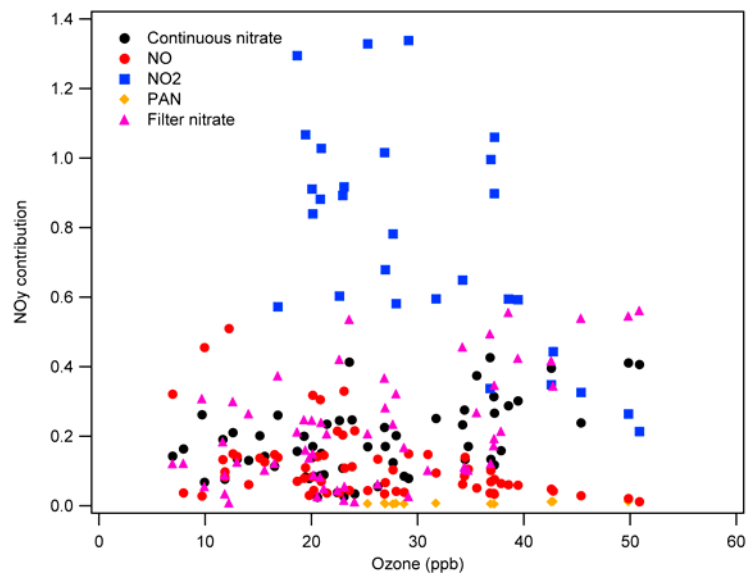


Figure 3-24. Relationship observed between the individual species contribution to  $\text{NO}_y$  and ozone at the Sierra Nevada Foothills site.

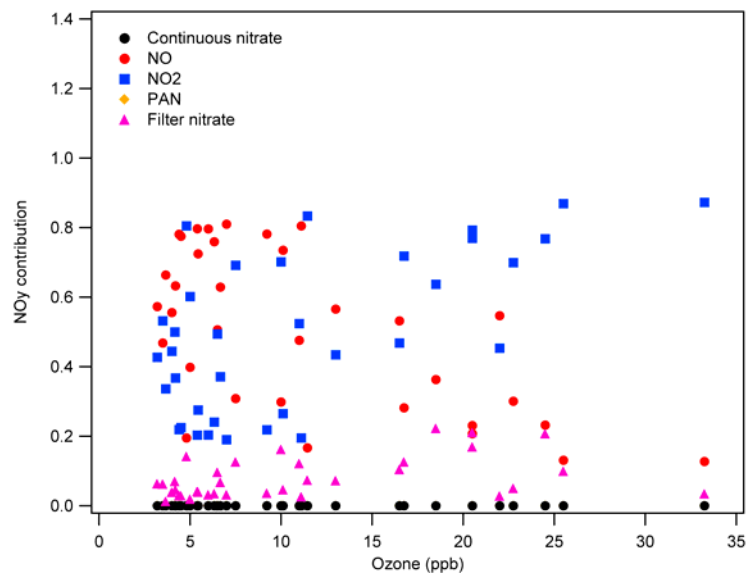


Figure 3-25. Relationship observed between the individual species contribution to  $\text{NO}_y$  and ozone at the Fresno site.

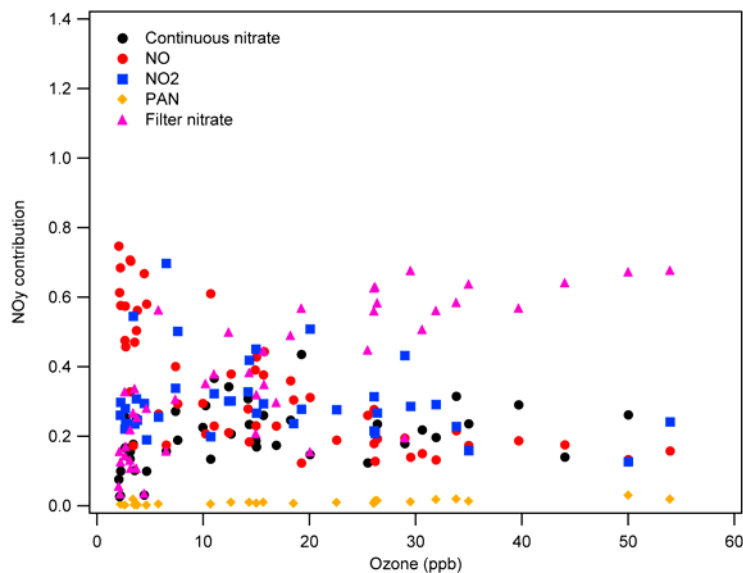


Figure 3-26. Relationship observed between the individual species contribution to  $\text{NO}_y$  and ozone at the Angiola site.

### 3.4.3 Light Scattering

**Figures 3-27 and 3-28** show the relationship observed between the  $\text{NO}_y(i)/\text{NO}_y$  ratios and light scattering at ANG and BTI. In this case, we might expect to see a positive relationship between nitrate and light scattering. That is the case for the filter nitrate measurements at ANG and both the filter and continuous nitrate measurements at BTI. In contrast, the continuous nitrate measurement at ANG shows a neutral to negative relationship with light scattering. Again, although it is not clear why the two measures of nitrate at ANG demonstrate such different relationships with the ancillary measures, it highlights the fact that the two nitrate measures are not responding to the same thing or one of the measurements is subject to significant artifacts.

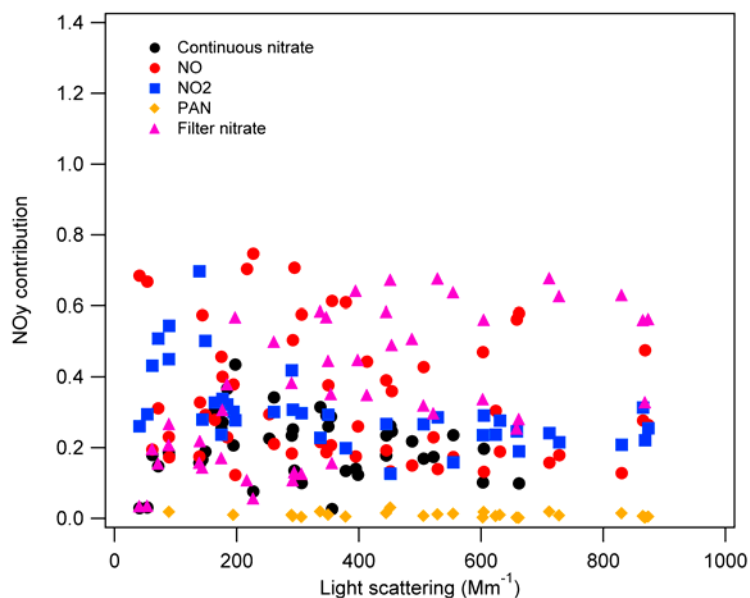


Figure 3-27. Relationship observed between the individual species contribution to  $\text{NO}_y$  and light scattering at the Angiola site.

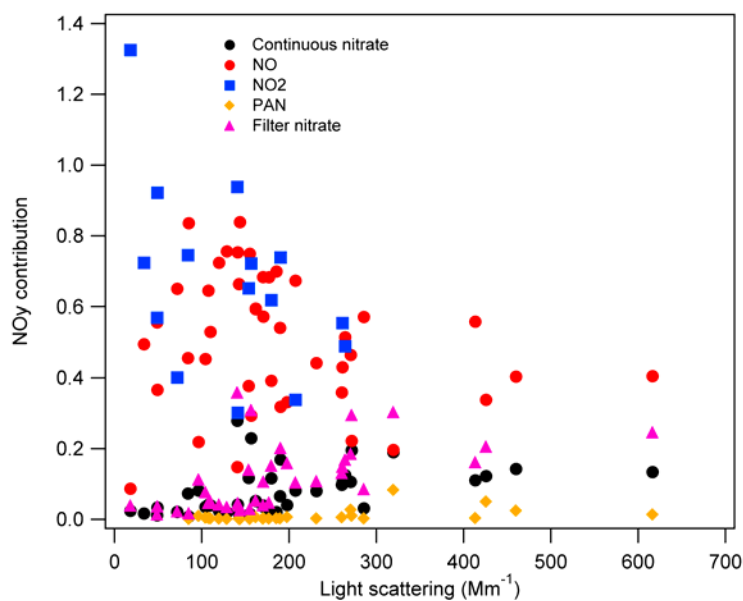


Figure 3-28. Relationship observed between the individual species contribution to  $\text{NO}_y$  and light scattering at the Bethel Island site.

### 3.5 DATA QUALITY ASSESSMENTS

Based on the level 2 data validation and analyses presented above, a data quality statement can be made for the different  $\text{NO}_y(i)$  species (see below). In general, these statements

are consistent with the level 1 data validation efforts summarized in the data quality summary reports (see (Hyslop et al., 2003).

### **3.5.1 NO**

The NO measurements collected at each of the sites appear to behave as expected within the reactive nitrogen family and should be used in other analysis without reservation.

### **3.5.2 NO<sub>2</sub>**

The NO<sub>2</sub> measurements collected using the GC/luminol system do not seem to represent the expected variability of NO<sub>2</sub> and should not be used in further analysis aimed at understanding chemical processes. The NO<sub>2</sub> measurements reported at the FSF site appear to behave as expected, but are subject to some artifact due to the universal NO<sub>x</sub> converter. Those NO<sub>2</sub> measurements might be useful as long as the measurement is understood as an upper limit for the true NO<sub>2</sub> concentration.

### **3.5.3 PAN**

The PAN measurements collected at some of the sites appear to behave as expected within the reactive nitrogen family and should be used in other analysis without reservation.

### **3.5.4 Nitrate**

Nitrate is possibly the most difficult reactive nitrogen species to measure individually. This is supported by the lack of good correlation between the collocated methods. In general terms, the filter-based nitrate data are commonly accepted as the most accurate measure of nitrate. The analysis presented here largely supports that contention and by extension that the filter nitrate data should be used in other analysis without reservation.

### **3.5.5 NO<sub>y</sub>**

The NO<sub>y</sub> measurements collected at each of the sites appear to behave as expected with respect to the reactive nitrogen family and should be used in other analysis without reservation.

#### 4. SUMMARY

Measurement of the individual components of  $\text{NO}_y$  and attempts to balance their sum with the  $\text{NO}_y$  measurement collected during CRPAQS was largely successful. In some cases, most notably the ANG and FSF data, the component parts and total measurement agreed quite well. In other cases the agreement ranged from poor to abysmal. However, the non-uniform  $\text{NO}_y$  partitioning story present in CRPAQS is not unique—only the most carefully coordinated independent measure of  $\text{NO}_y$  species result in better understanding the  $\text{NO}_y$  family. Each site presents a data set that has enormous value, both in the individual species measurements and their relationship to each other. A caution is applicable to the  $\text{NO}_2$  measurements at all sites, but particularly where the measurement was made with the luminol-based detector (see Section 3.5.2). In contrast, the results presented here suggest that the measurements of  $\text{NO}$ ,  $\text{NO}_y$  (where executed with an inlet-based converter), filter nitrate, and PAN can be used with reasonable measurement uncertainty expectations.



## 5. REFERENCES

- Buhr M.P., Parrish D.D., Norton R.B., Fehsenfeld F.C., Sievers R.E., and Roberts J.M. (1990) Contribution of organic nitrates to the total reactive nitrogen budget at a rural eastern U.S. site. *J. Geophys. Res.* **95** (D7), 9809-9816.
- Hering S.V. (2004) Aerosol Dynamics, Inc., Berkeley, CA. Personal communication with M.P. Buhr, Sonoma Technology, Inc., Petaluma, CA, March.
- Hyslop N.P., Brown S.G., Gorin C.A., and Hafner H.R. (2003) California Regional PM<sub>10</sub>/PM<sub>2.5</sub> Air Quality Study (CRPAQS) data quality summary reports. Final report prepared for San Joaquin Valleywide Air Pollution Study Agency c/o California Air Resources Board, Sacramento, CA, by Sonoma Technology, Inc., Petaluma, CA, STI-999242-2310-FR, February. Available on the Internet at <http://www.arb.ca.gov/airways/Documents/preliminary/STI/STIDQSR.pdf> last accessed November 22, 2004.
- Trainer M., Buhr M.P., Curran C.M., Fehsenfeld F.C., Hsie E.Y., Liu S.C., Norton R.B., Parrish D.D., Williams E.J., Gandrud B.W., Ridley B.A., Shetter J.D., Allwine E.J., and Westberg H.H. (1991) Observations and modeling of the reactive nitrogen photochemistry at a rural site. *J. Geophys. Res.* **96** (D2), 3045-3063.